

On Multi-Robot Path Planning Based on Petri Net Models and LTL specifications

Sofia Hustiu, Cristian Mahulea, Marius Kloetzer, and Jean-Jacques Lesage

Abstract—This work considers the path planning problem for a team of identical robots evolving in a known environment. The robots should satisfy a global specification given as a Linear Temporal Logic (LTL) formula over a set of regions of interest. The proposed method exploits the advantages of Petri net models for the team of robots and Büchi automata modeling the specification. The approach in this paper consists in combining the two models into one, denoted *Composed Petri net* and use it to find a sequence of action movements for the mobile robots, providing collision free trajectories to fulfill the specification. The solution results from a set of Mixed Integer Linear Programming (MILP) problems. The main advantage of the proposed solution is the completeness of the algorithm, meaning that a solution is found when exists, this representing the key difference with our previous work in [1]. The simulations illustrate comparison results between current and previous approaches, focusing on the computational complexity.

Index Terms—High-level specifications, formal methods, Petri nets, autonomous robots

I. INTRODUCTION

The significance of developing path planning methods for a team of mobile robots has been intensified in the last years. Many researchers propose different approaches, based on various representations which capture the robots movements in the environment such as transition systems [2], [3] or Petri net models [4], [5]. In multiple scenarios, the robots are required to fulfill a defined global goal. The most used formalisms to express missions for the team of robots are based on high-level specification, such as: Boolean specifications [6] and Linear Temporal Logic (LTL) specifications [7]. The motion planning must ensure the given mission by computing collision free trajectories for the team members.

Certainly, the association between the environment model and the specification one can be computed in various ways to return *the best* solution for a considered scenario. In previous works, one can notice the complexity drawback of the centralized approach based on transition system representations. Thus, for large teams of robots, the discrete centralized model used to solve the path planning problem generates an exponential increase of the discrete states with respect to the number of robots. This is due to the fact that the centralized model is obtained by the synchronous product

of a number of transition systems equal to the number of robots, each transition system capturing the evolution of a robot. Additionally, the resulted model is further extended by doing the synchronous product with the Büchi automaton modeling the specification. To overcome this complexity issue, in [2], the path planning is computed by assuming a different transition system for each robot and the global specification is *distributed* into individual tasks. Each individual task is solved using the transition system of only one robot, hence with a smaller number of states than the centralized model. However, not all LTL formulas can be distributed and the distribution algorithm has a high computational complexity.

Another approach to overcome the centralized solution using transition system models is based on using a Petri net model of the environment [1]. The structure of this Petri net model is independent with respect to the number with robots, since the robots are represented by the tokens. Therefore, the models used in the work [1] are: a Petri net model for the team and the Büchi automaton for the LTL formula. Then, a set of k runs in the form of *prefix* and *suffix* in Büchi automaton is computed by using the k -shortest path algorithm. The next step is to take a run and try to follow it by obeying the PN model structure. If the run cannot be followed because the observations cannot be generated by the robots or the observations can generate other transitions in Büchi, the procedure considers another run and iterates the algorithm. The main problem of this approach is that the algorithm is not complete and it cannot ensure that a solution is obtained (if there exists), but also a set of k runs should be computed.

The main contribution of the current work is to propose a complete algorithm which ensures the attainment of a solution when this is achievable (expressed as collision free robot trajectories). For this reason, the technique aims to use both Petri net model and Büchi automaton in a joined model denoted *Composed Petri net* model. The new model exploits the search of an accepted run in Büchi while providing feasible independent trajectories in a reduced Quotient Petri net model of the environment. The latter representation decreases the size of the original PN model, considering one place for each unique observation. The complete solution is returned as a result of two MILPs: (1) for joined model denoted *Composed Petri net* model and (2) to project the solution in the original PN model. Furthermore, the complexity of this work depends on the total number of places of the joined model represented by a sum and not a Cartesian product, e.g., automaton product [8].

The paper follows the next structure: Section II captures several approaches in the field of robot motion planning, revealing the current challenges based on the related work. Section III asserts the problem definition, while Section IV

S. Hustiu and M. Kloetzer are with the Dept. of Automatic Control and Applied Informatics, Technical University “Gheorghe Asachi” of Iasi, Romania {{hustiu.sofia,kmarius}@ac.tuiasi.ro}.

C. Mahulea is with the Aragón Institute of Engineering Research (I3A), University of Zaragoza, Maria de Luna 1, 50018 Zaragoza, Spain {cmahulea@unizar.es}.

J.J. Lesage is with Université Paris-Saclay, ENS Paris-Saclay, LURPA, 91190, Gif-sur-Yvette, France {jean-jacques.lesage@ens-paris-saclay.fr}

The work of C. Mahulea has been partially supported by the MINECO “Salvador de Madariaga” program. This work has been partially supported by CICYT-FEDER project PID2021-125514NB-I00 at University of Zaragoza.

seizes the mathematical notations used alongside the paper. The complete solution partitioned into its two main steps is explained in Sections V, VI, joined by examples. Section VII is dedicated to the analysis of the results based on several numerical simulations. Also, a comparison with an existing sequential method is illustrated. The last section exposes the conclusions of the current work, while mentioning future improvements.

II. RELATED WORK

Path planning for mobile robots started by analysing various methods to reach a given destination point from an initial point, especially for single robot scenario [9]. As the problem is extended towards multi-robot navigation, the focus is directed to concepts such as: (1) type of approach - centralized, decentralized, distributed; (2) the problem formulation based on global or individual mission given for the team of robots.

High-level specifications can be used to specify the mission for a team of robots (which are usually denoted as *agents* to enlarge the aim of the proposed method in other areas). It is often assumed that the robots are identical. One intuitive language is represented by Linear Temporal Logic (LTL), encoding human representation into a logical and temporal formalism, e.g., “visit region A, then region B and always avoid region C”. Any LTL specification can be modeled as a Rabin automaton [10], or a Büchi automaton [1] for example. In addition, this formalism is efficient in defining a global mission for the entire team [11], [12], or local mission for each agent [13]. The LTL formalism is effective also to plan optimal motion trajectories [14]. In [11], the global LTL mission is decomposed into individual independent tasks, for a flexible centralized approach of task assignment with respect to the robots. This work was extended afterwards in the 3D space, for a team of Unmanned Aerial Vehicles (UAVs) [12]. On the other hand, the paper [13] is directed to solve the path planning problem by assigning individual LTL tasks for each robot. The robots cooperate while satisfying hard (for collision free trajectories) and soft LTL constraints. The notion of LTL soft and hard constraints is also included in others works, e.g., [15].

There are various mechanisms to combine the LTL specification model with the representation of the dynamic robotic system. One approach is based on transition system models, based on a partitioned environment (defining the nodes) and their adjacency relation (defining the edges) [16]. In [3], the authors use the transition system model for a group of mobile robots, with individual scope given for each robot. A different approach is illustrated in [17], where the nodes illustrate the kinematic of individual agents and the edges capture the inter-agent constraints. All of these approaches encounter the same disadvantage as a result of using the transition system to model the dynamic robotic system, this being expressed as the exponential increase of complexity. This is the result of automaton products [8]. To overcome this downside, the paper [2] reduces the complexity of multi-robot path planning by considering the following: decomposing the problem into multiple finite horizon planning issues, and solving them in iterative manner, using an event-based synchronization between agents.

Another solution to overcome the state explosion problem is by using another representation for the motion of the robots in the workspace, such as Petri net (PN) model. Considering a given environment, PN model has a fixed topology subject to the number of robots, and is easily adaptable related to their initial position. In [6] the collision free trajectories of robots are obtained as a result of solving two Mixed Linear Integer Programming (MILP) problems, while the environment is modeled as a PN and a Boolean specification is given. The approach used in [18] consists in the use of three layered PN model which represent the environment, the changes in the work-space, and the task plan based on the compositions different types of events and actions towards goal.

The benefits of the Petri net models are illustrated also in works which consider unknown or partially known environment, e.g., [4] - the robots need to avoid regions which have a high probability of collision, while satisfying a Boolean specification, without knowing their precise location.

So far we have presented the benefits of using both models to achieve collision free trajectories while a given specification should be fulfilled: PN models for the dynamic robotic system and LTL specification for the team’s mission. A “high-level” view of mobile planning can be catalogued as follows: in [19] a PN model is assigned to each robot, ensuring a global LTL mission; in [20] - each robot is modeled as an automaton, being supervised periodically; in [21] - capturing the notion of supervisory control, where a framework for multi-robot system is enforced.

On the other hand, from a “low-level” point of view it is observed that is not easy to design a controller for a team of agents satisfying a given mission. Several works exploit these models separately, omitting some advantages which could appear by using both models in the same time. One such example is proposed in paper [21] considering a parallel execution of transitions in the PN model (of the workspace) and the Büchi automaton (of the LTL formula), based on the construction of a new PN supervisor model. In other words, one transition in the environment model is fired only if a transition in the Büchi automaton is satisfied. The authors mention that is difficult to design a PN supervisory model for complex tasks, the construction being prone to errors especially without having a formal method of verification. We proposed a different approach in a previous work [1]: the Büchi automaton and the PN model are used sequentially compared with the parallel approach from [21]. Herein, a single run in the Büchi automaton is pursued, followed by a sequence of the robots in the PN model with respect to the selected run. The procedure is iterated until the robots meet the LTL specification. While the results demonstrate the benefit of this approach, the proposed algorithm is not complete.

With this work we propose a method based on a joined *Composed Petri net* model. In this sense, a Quotient PN model is computed with respect to the original PN model of the environment, where each place models an unique observation. The reduced model of the dynamic robotic system is afterwards combined with the Büchi automaton. The movement sequence for the team of robots is returned by the solution of two MILPs (based on the reduced model and a projection in the

original PN model), their trajectories satisfying a global LTL specification. To the best of our knowledge, this composition of Petri net and Büchi automaton was never done before to solve such path planning problems. The proposed algorithm is complete, while the complexity increase is reduced due to a smaller number of places in the joined Petri net model. Compared with other approaches based on automaton product which suffer from an exponential increase in the number of states, the design of *Composed Petri net* model handles a number of places equal to a sum between places in the Quotient PN, number of states in Büchi automaton and twice the number of individual observations.

III. PROBLEM STATEMENT

Let us consider the next problem definition: a set of identical robots denoted $R = \{r_1, r_2, \dots, r_{|R|}\}$ evolves in an known and static 2D environment. The robots are assumed omnidirectional and of negligible size, i.e., each is a fully actuated point. The environment captures several convex polygonal shapes, denoted as regions of interest (ROI) and labeled with elements from the set $\mathcal{Y} = \{y_1, y_2, \dots, y_{|\mathcal{Y}|}\}$. These regions can be both disjointed and overlapped. Furthermore, based on these polygonal shapes, we assume that the environment is partitioned into a set of regions also called cells, for example by using a cell decomposition method [16], [22]. Each cell entirely belongs to the same region(s) of interest, or it is included in the area not covered by any region of interest (free space). The advantage of this representation lies in obtaining an abstract model of the environment, e.g., Petri net model, which captures the entire space data, being invariant with respect to the number of robots.

The set of cells is denoted by $P = \{p_1, p_2, \dots, p_{|P|}\}$ and the set of labels assigned to a cell is given by a function $h : P \rightarrow \mathcal{Y} \cup \{\emptyset\}$. If the cell p_i is included in the intersection of ROIs y_j and y_k , then $h(p_i) = \{y_j, y_k\}$, while if p_i lies in the free space, then $h(p_i) = \emptyset$. Fig. 1(a) can be used as example for an intuitive illustration.

Problem 3.1: Assume that the movement of a robotic team is abstracted to a Robot Motion Petri Net (RMPN) model given in Def. 4.1. Given a global LTL specification over the set \mathcal{Y} , automatically compute trajectories for the robots in order to fulfill the specification.

Example 3.2: Let us consider the following mission task for the robots in Fig. 1(a):

$$\varphi = \diamond (y_1 \wedge y_2 \wedge y_3) \wedge \neg (y_1 \vee y_2) \mathcal{U} (y_1 \wedge y_2) \quad (1)$$

This task means that regions y_1 , y_2 and y_3 should be *eventually* visited at the same time, and y_1 and y_2 should be reached simultaneously. ■

The main idea proposed in [1] computes an accepted run in the Büchi automaton B , and then searches trajectories in the RMPN in order to sequentially generate observations that follow the imposed run of B . However, when the trajectories are computed in the RMPN, some other observations can be generated that could produce a transition in B that deviates from the imposed run. In this case, the procedure is iterated by imposing another accepted run in Büchi and then try to follow

it with RMPN's outputs. For this approach, several Mixed Integer Linear Programming (MILP) optimization problems were solved. The algorithmic strategy in [1] is not complete, and it does not account for collision free trajectories, aspects that are solved by the strategy herein, in this paper.

In the following sections we proposed a different solution than the one in [1] which can be divided in two steps. First, we derive a PN model in which we embed an abstraction (Quotient) of RMPN with the Büchi automaton B , denoted *Composed Petri net* model. In the second step, a run is found in the new joined Petri net model, with the property of being feasible, while generating a sequence of outputs accepted by B . The obtained run is projected on the original RMPN and the robot trajectories are computed.

For each step in the next sections, the paper is accompanied by mathematical notations and examples, for an easier understating of the proposed algorithm.

IV. NOTATIONS AND PRELIMINARIES

Definition 4.1: [16] A Robot Motion Petri Net system (RMPN) is a tuple $\mathcal{Q} = \langle \mathcal{N}, \mathbf{m}_0, \mathcal{Y}, h \rangle$, where:

- $\mathcal{N} = \langle P, T, \mathbf{Post}, \mathbf{Pre} \rangle$ is a Petri net with:
 - The set of places P (one place for each cell);
 - Set of transitions T , each transition corresponding to a robot movement between adjacent cells;
 - $\mathbf{Post} \in \{0, 1\}^{|P| \times |T|}$ is the post-incidence matrix, defining the arcs from transitions to places, with $\mathbf{Post}[p, t] = 1$ if $t \in T$ is connected with place $p \in P$, otherwise $\mathbf{Post}[p, t] = 0$;
 - $\mathbf{Pre} \in \{0, 1\}^{|P| \times |T|}$ is the pre-incidence matrix defining the arcs from places to transitions, with $\mathbf{Pre}[p, t] = 1$ if place $p \in P$ is connected with transition $t \in T$, otherwise $\mathbf{Pre}[p, t] = 0$;
- \mathbf{m}_0 is the initial marking, where $\mathbf{m}_0[p]$ gives the number of robots initially deployed in cell $p \in P$;
- $\mathcal{Y} \cup \{\emptyset\}$ is the set containing the output symbols;
- $h : P \rightarrow \mathcal{Y} \cup \{\emptyset\}$ is the observation map, defined above. Thus, if p_i has at least one token (i.e., at least one robot is currently in cell p_i), then region(s) of interest $h(p_i)$ is (are) visited.

Example 4.2: Let us consider the environment in Fig. 1(a), containing three ROIs ($\mathcal{Y} = \{y_1, y_2, y_3\}$) and two robots, initially located in p_2 and p_{20} . Therefore, $h(p_{11}) = h(p_{23}) = y_1$, $h(p_{17}) = h(p_{18}) = h(p_{24}) = h(p_{26}) = y_2$, $h(p_4) = h(p_{10}) = y_3$, $h(p_{13}) = \{y_1, y_2\}$, and $h(p_i) = \emptyset$ otherwise.

The RMPN modeling the movement capabilities of this team of two robots consist in a set of 26 places and 74 transitions. The set of outputs \mathcal{Y} and the observation map h are given before. The initial marking \mathbf{m}_0 is a vector of dimension 26 having all elements equal to zero except $\mathbf{m}_0[p_2] = \mathbf{m}_0[p_{20}] = 1$. ■

Each token in the RMPN models the current location (cell) of each robot, hence the total number of tokens is equal to $|R|$. Notice that by using this definition, the structure of the model (number of places, transitions and arcs) is not changing

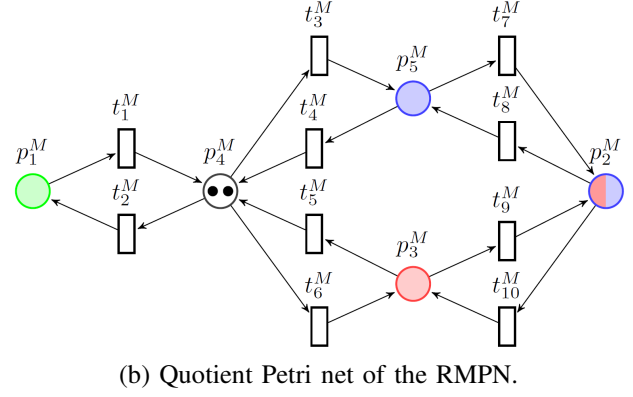
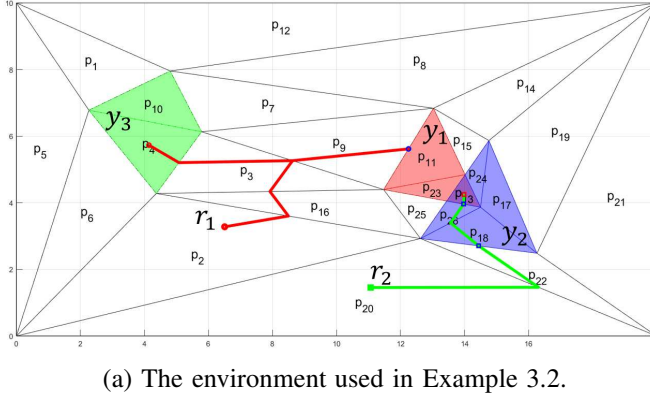


Fig. 1: Example of an environment and the corresponding RMPN's quotient.

if robots identical with others are added (removed) to (from) the team. Only the marking (state) of the RMPN is changed.

For a generic transition $t_j \in T$, $\bullet t$ denotes its input place, while t^\bullet denotes its output place¹. An enabled transition t_j can fire, and the RMPN reaches a new marking $\tilde{m} = m + C[\cdot, t_j]$, where $C = \text{Post} - \text{Pre}$ is the token flow matrix and $C[\cdot, t_j]$ is its column corresponding to t_j . Based on the construction of the RMPN, the firing of a transition t_j corresponds to the movement of a robot from cell $\bullet t_j$ to cell t_j^\bullet . For the moving robot, transition t_j means to apply a control law that drives the robot from cell $\bullet t_j$ to t_j^\bullet , and there exist approaches for designing such continuous laws in specific scenarios [23], [24].

We will be interested in finding sequences of transitions to be fired such that the team fulfills a given specification. If a RMPN marking \tilde{m} can be reached from m through a finite sequence of transitions σ , we denote with $\sigma \in \mathbb{N}_{\geq 0}^{|T|}$ the firing count vector, i.e., its j^{th} element is the cumulative amount of firings of t_j . In this case, the state (or fundamental) equation is satisfied:

$$\tilde{m} = m + C \cdot \sigma \quad (2)$$

A firing vector σ can be found, having a minimum number of transitions that drives the live² RMPN to a desired marking \tilde{m} , i.e., by solving the optimization problem $\min 1^T \cdot \sigma$. The details of transforming the firing vector into a sequence of robot movements are captured in [16].

LTL formulae and Büchi automata The global motion task that the robot team should fulfill is specified as an LTL_{-X} formula [25], [26]. The subclass of LTL denoted as LTL_{-X} contains formulae recursively defined over a set of atomic propositions \mathcal{Y} , by using the standard Boolean operators (\neg - negation, \wedge - conjunction, \vee - disjunction, \Rightarrow - implication, and \Leftrightarrow - equivalence) and some temporal operators (\mathcal{U} - until, \diamond - eventually, and \square - always). For simplicity of notation we further write LTL instead of LTL_{-X} , the difference being the absence of the next operator \bigcirc in LTL_{-X} [27], [28], [26].

¹By definition, RMPN systems considered in this paper belongs to the class of state-machine, i.e., each transition has one input and one output place.

²A Petri net is live if independently by the actual reachable marking, all transitions can fire in the future.

As proved in [29], any LTL formula can be transformed into a non-deterministic Büchi automaton that accepts all and only the input strings satisfying the formula. Automatic translation from an LTL formula to Büchi automaton can be done by using available tools, for example [30], [31], [32]. The property of LTL being close under stuttering [33] is exploited in the paper. This means that any finite repetition of the same input does not modify the truth value of the input string. The stuttering is useful in Section VI, when the obtained solution in the reduced Quotient Petri net model is projected into the original RMPN.

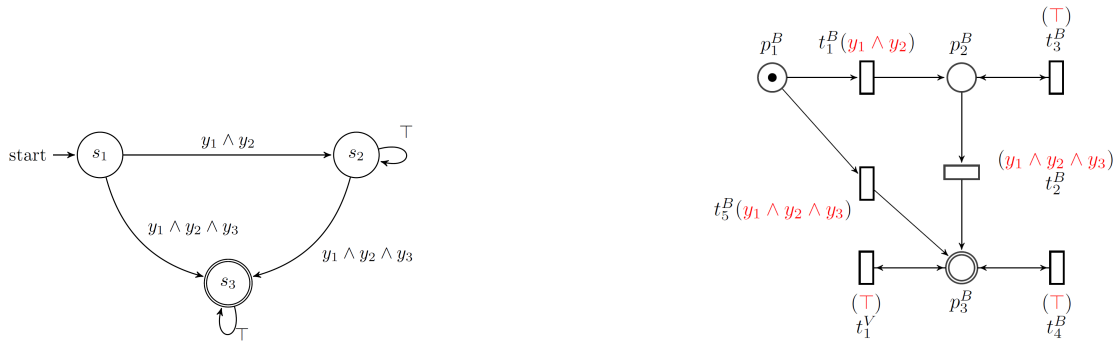
Definition 4.3: The Büchi automaton corresponding to an LTL formula over the set \mathcal{Y} has the structure $B = (S, S_0, \Sigma_B, \rightarrow_B, F)$, where:

- S is a finite set of states;
- $S_0 \subseteq S$ is the set of initial states;
- Σ_B is the finite set of inputs;
- $\rightarrow_B \subseteq S \times \Sigma_B \times S$ is the transition relation;
- $F \subseteq S$ is the set of final states. ■

B can be non-deterministic, by means of enabling multiple outgoing transitions from the same input state, e.g., $(s, \tau, s') \in \rightarrow_B$ and $(s, \tau, s'') \in \rightarrow_B$, with $s' \neq s''$. We denote by $\pi(s_i, s_j)$ the set of all inputs that enable transition from s_i to s_j , expressed as a Boolean formula over the set \mathcal{Y} , reduced to a Disjunctive Normal Form (DNF). The input can be also expressed as combination of active observations over the set $2^{\mathcal{Y}}$, where \emptyset represents the free space. To reduce the complexity in the proposed algorithm, the selected formulation is based on Boolean formulae, where a single conjunctive element is denoted with α_k .

An *infinite accepted run* in B drives the automaton towards a final state from an initial state. This run can be stored on finite memory with regards to two finite length strings (i) *prefix* - towards a final state in set F ; (ii) *suffix* - towards the same final state reached by the prefix. The run can be written as *prefix, suffix, ...* More about infinite runs in B , joined by computing the sequence of elements from Σ_B can be found in [29].

Example 4.4: Let us recall the Example 3.2. The Büchi automaton corresponding to this LTL task is given in Fig. 2(a), where symbol \top (True) means any observation from $2^{\mathcal{Y}}$. On the other hand, Fig. 2(b) illustrates the Büchi Petri net model, having the Boolean formula of transitions represented



(a) Büchi automaton for the LTL formula in Ex. 3.2. (b) Büchi Petri net corresponding to the Büchi automaton in Fig. 2(a)

Fig. 2: Example of Büchi automaton and Büchi Petri net

with red color. This model will be described in Section V. An accepted run satisfying the formula could be s_1, s_3, s_3, \dots with prefix s_1 and suffix s_3 . Notice that the unique final state s_3 is visited infinitely often. However, as it may be observed in the environment of Fig. 1(a), this run cannot be generated by the two robots. Indeed, the input necessary for the first run's transition of is $\pi(s_1, s_3) = y_1 \wedge y_2 \wedge y_3$, which cannot be generated when starting from the initial location of the robots (p_2 and p_{20}). This is because the two robots should evolve only through cells belonging to free space until one enters p_{13} and the other simultaneously enters p_4 or p_{10} . Clearly, entering in p_{13} directly is not possible since it would require to activate first y_1 or y_2 and would violate φ .

A possible run that can be generated by the robots is: $s_1, s_2, s_3, s_3, \dots$ with prefix s_1, s_2 and suffix s_3 . For this, the robots should first enter in y_1 and y_2 synchronously (generating $\pi(s_1, s_2) = y_1 \wedge y_2$), then one robot should go to p_{13} (the intersection of y_1 and y_2). After this, the other robot will move to the free-space, and the output generated by the team remains in y_1, y_2 , no matter in what cell from free-space is located the second robot. Finally, the robot from the free-space should enter to y_3 , the team generates output $\pi(s_2, s_3) = y_1 \wedge y_2 \wedge y_3$, and the transition to s_3 in Büchi automaton is enabled. The robots can stop in these final regions since the self-loop in s_3 includes all possible observations.

Let us remark that the solution is not unique, since the self-loop transition in s_2 can be taken with any possible input. In particular, the robot that is going to p_{13} can wait in the previous cell and enter in p_{13} synchronously with the other robot in y_3 . The above intuitive explanations lead to the idea of automatically obtain a team movement strategy which satisfies the LTL formula, thus formulating the problem we solve. ■

Various notations are used in describing the proposed algorithm for the complete solution, divided into several steps. These symbols are significant when expressing the tuple \mathcal{Q} for RMPN, next to its components. The Table I captures a summarized description for an established overview. In this sense we propose a general notation for all the components denoted as $\langle \cdot \rangle$, accompanied by different symbols for different topics. The detailed explanations are included in each section alongside the introduced equations and pseudo-codes.

Notation	Description
$\langle \cdot^M \rangle$	Denotes the variables used for Quotient RMPN (Sub-step 1.1)
$\langle \cdot^B \rangle$	Denotes the variables used for Büchi RMPN (Sub-step 1.2)
$\langle \cdot^C \rangle$	Denotes the variables used for Composed Petri net (Sub-step 1.3)

TABLE I: Notations for various PNs to be used

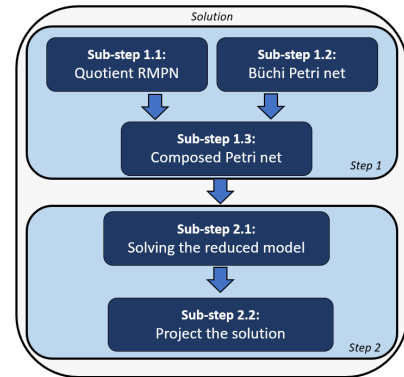


Fig. 3: Diagram for the global algorithm

V. SOLUTION STEP 1: FULL PETRI NET MODEL

Fig. 3 captures the steps and sub-steps of the method we propose to achieve the final solution to the stated Problem 3.1. The first phase is responsible to output the full Petri net model. In this sense, two Petri net models are assigned to (i) the environment (Sub-step 1.1) - considering a reduced abstraction of the entire space denoted Quotient Petri net and to (ii) the LTL specification (Sub-step 1.2) - based on the Büchi automaton. The composition of these models is performed (Sub-step 1.3) in a reduced representation which accounts the active observations while ensuring the given specification. The second phase focuses on the final solution. For this, two actions are required: Sub-step 2.1 returns the solution based on the *Composed Petri net* model, while Sub-step 2.2 projects this solution into a sequence of robot trajectories.

In this section we employ first a *Quotient* model of the RMPN presented in [34] that is obtained by aggregating adjacent cells with identical observations.

Sub-Step 1.1. Quotient of the RMPN in Def. 4.1. Given a RMPN system \mathcal{Q} as in Def. 4.1, the idea of obtaining the quotient \mathcal{Q}^M is to iteratively combine any places p_i and p_j from P that satisfy $p_j \in (p_i^\bullet)^\bullet$ and $h(p_i) = h(p_j)$. This reduction technique is synthesized in Alg. 1, and the reduced PN model \mathcal{Q}^M has the property that its output is updated when a transition is fired. Therefore, after the firing of one transition in \mathcal{Q}^M , one transition in Büchi should be fired too. Moreover, since a transition of \mathcal{Q}^M corresponds to a set of trajectories in \mathcal{Q} , any sequence of transition firings in \mathcal{Q}^M can be translated to a run in \mathcal{Q} .

The main loop in Alg. 1 (lines 4 - 13) is iterated until there exist no adjacent places with the same observation. In each iteration, for any pair of adjacent places $\langle p_i^M, p_j^M \rangle$ with the same observation, the two transitions t_k^M and t_l^M modeling the movements of a robot from p_i^M to p_j^M and from p_j^M to p_i^M are removed (lines 5 - 7). Then, p_i^M and p_j^M are fused in p_i^M by updating the marking vector, the incidence matrices (lines 8 - 11) and the projection matrix \mathbf{Pr} (lines 12 - 13).

Example 5.1: Let us consider the RMPN for the environment captured in Fig. 1(a). By aggregating the states with the same observation (applying Alg. 1), the Petri net system \mathcal{Q}^M in Fig. 1(b) is obtained. This new PN model is also a RMPN according to Def. 4.1, where each place corresponds to a set of regions in the original RMPN system. Notice that Alg. 1 also returns the projection matrix \mathbf{Pr} , in this case of size 5×26 and having all elements equal to zero except the following:

- $\mathbf{Pr}[p_1^M, p_4] = \mathbf{Pr}[p_1^M, p_{10}] = 1$ saying that place p_1^M combines p_5 and p_{10} ;
- $\mathbf{Pr}[p_3^M, p_{11}] = \mathbf{Pr}[p_3^M, p_{23}] = 1$;
- $\mathbf{Pr}[p_5^M, p_{17}] = \mathbf{Pr}[p_5^M, p_{18}] = \mathbf{Pr}[p_5^M, p_{24}] = \mathbf{Pr}[p_5^M, p_{26}] = 1$;
- $\mathbf{Pr}[p_2^M, p_{13}] = 1$;
- $\mathbf{Pr}[p_4^M, p_i] = 1$ for all $p_i \in P$ with $h(p_i) = \emptyset$. ■

Sub-Step 1.2. Büchi Petri net. Starting from the Büchi automaton $B = \langle S, S_0, \Sigma_B, \rightarrow_B, F \rangle$ as in Def. 4.3, Alg. 2 obtains the corresponding Büchi Petri net system \mathcal{Q}^B . For each state $s_i \in S$, a new place p_i^B is added to the PN (line 1). The first loop (lines 3 - 8) is executed for each transition from a s_i to a s_j in the Büchi automaton. The second loop (lines 4 - 8) is executed for each conjunctive element α_k from $\pi(s_i, s_j)$ and is adding a new transition t_{τ_k} in the Büchi Petri net from p_i^B to p_j^B . Notice that all transitions corresponding to the conjunctive elements in $\pi(s_i, s_j)$ have the same input and the same output place from the Büchi PN. In line 9, the marking vector is initialized and it is updated in the loop in lines 10 - 11. In particular, for each initial state of the Büchi automaton, one token is added in the corresponding place.

Alg. 2 returns also *virtual transitions* T^V , their relation with the final states being captured in \mathbf{Pre}^V and \mathbf{Post}^V . These transitions will have zero firing cost when the solution of MILP (3) is computed (explained in the next section) to maintain the Büchi PN in the final state if possible. One virtual transition is assigned to each final state s_f of Büchi PN.

Example 5.2: Let us consider the Büchi automaton in Fig. 2(a). By applying Alg. 2, the Büchi PN in Fig. 2(b) is obtained. In this example, the places p_2^B and p_3^B matching states s_2 and s_3 are connected with a single transition corre-

Algorithm 1: Quotient of RMPN system

Input: $\mathcal{Q} = \langle \langle P, T, \mathbf{Pre}, \mathbf{Post} \rangle, m_0, \mathcal{Y}, h \rangle$

Output: $\mathcal{Q}^M = \langle \langle P^M, T^M, \mathbf{Pre}^M, \mathbf{Post}^M \rangle, m_0^M, \mathcal{Y}, h \rangle, \mathbf{Pr}$

- 1 $P^M = P$; $T^M = T$;
 - 2 $\mathbf{Pre}^M = \mathbf{Pre}$; $\mathbf{Post}^M = \mathbf{Post}$; $m_0^M = m_0$;
 - 3 $\mathbf{Pr} = \mathbf{I}^{|P| \times |P|} / \star$ \mathbf{Pr} is the projection matrix */
 - 4 **while** $\exists p_i^M, p_j^M \in P^M$ such that $p_j^M \in (p_i^M)^\bullet$ and $h(p_i^M) = h(p_j^M)$ **do**
 - 5 Let $t_k^M = p_i^M \bullet \cap \bullet p_j^M$ and $t_l^M = \bullet p_i^M \cap p_j^M \bullet$;
 - 6 Remove columns corresponding to t_k^M and t_l^M from \mathbf{Pre}^M and \mathbf{Post}^M ;
 - 7 $T^M = T^M \setminus \{t_k^M, t_l^M\}$;
 - 8 $m_0^M[p_i^M] = m_0^M[p_i^M] + m_0^M[p_j^M]$;
 - 9 Remove row p_j^M from \mathbf{Pre}^M and \mathbf{Post}^M ;
 - 10 Remove element p_j^M from m_0^M ;
 - 11 $P^M = P^M \setminus \{p_j^M\}$;
 - 12 $\mathbf{Pr}[p_i^M, \cdot] = \mathbf{Pr}[p_i^M, \cdot] + \mathbf{Pr}[p_j^M, \cdot]$;
 - 13 Remove row p_j^M from \mathbf{Pr} ;
-

sponding to input $\pi(s_2, s_3) = y_1 \wedge y_2 \wedge y_3$. Near the transition labels it is written the input for Büchi that is required in order to fire the transition. Fig. 2(b) illustrates the addition of the virtual transition t_1^V connected with the final state s_3 by a bi-directional arc. Once the system reaches this final state following the *prefix*, the system persist in this state without additional cost in the proposed MILP. ■

Sub-Step 1.3. Composition of Quotient RMPN and Büchi Petri net systems. Alg. 3 includes the full strategy to return a PN system \mathcal{Q}^C , by composition of the robotic team model (\mathcal{Q}^M from Alg. 1) with the one of the specification (\mathcal{Q}^B from Alg. 2). For this, a number of $2 \times |\mathcal{Y}|$ places are needed, from which a half models the active observations (added in line 1), while the other $|\mathcal{Y}|$ places model inactive observations (added in line 2). Next line 3 puts zero tokens in the places modeling active observation places since we assume no active observation at the initial marking. In contrast, a number of tokens equal with the number of robots, i.e., $|R|$, are added to the inactive observations places. The sum of tokens in p_i^{-O} and p_i^O is always equal to $|R|$. In line 4, Alg. 1 is called to compute the \mathcal{Q}^M , while line 5 call Alg. 2 to compute the \mathcal{Q}^B . The next lines (6 - 7) define the sets of places, respectively transitions for the *Composed PN* system \mathcal{Q}^C , while line 8 defines the initial marking.

The matrices \mathbf{Pre}^C and \mathbf{Post}^C are initialized in lines 9 - 10. The last part of Alg. 3 is responsible to combine the Quoting PN with Büchi Petri net by using the places modeling active and inactive observations. The loop in lines 11 to 15 is executing for each observation y_i . For each place p_k of the Quoting PN with output y_i , i.e., $y_i \in h(p_k)$, arcs from all input transitions to p_k to place p_i^O are added. Additionally, arcs from p_i^O to all output transitions of p_k are added as well. In this way, when a robot is entering in a region p_k with output

Algorithm 2: Büchi Petri net

Input: $B = \langle S, S_0, \Sigma_B, \rightarrow_B, F \rangle$
Output: $Q^B = \langle \langle P^B, T^B \cup T^V, [Pre^B \ Pre^V], [Post^B \ Post^V] \rangle, m_0^B, \mathcal{Y}, h \rangle$

- 1 Let $P^B = \{p_1^B, p_2^B, \dots, p_{|S|}^B\}$ be the set of $|S|$ places;
- 2 Let $T^B = \emptyset$ and $T^V = \emptyset$;
- 3 **forall** $(s_i, \tau, s_j) \in \rightarrow_B$ **do**
- 4 **forall conjunctive element** α_k **of** $\pi(s_i, s_j)$ **do**
- 5 $T^B = T^B \cup t_{\tau_k} / *$ add a new transition to T^B */
- 6 Add a new column to Pre^B and to $Post^B$ corresponding to t_{τ_k} ;
- 7 $Pre^B[p_i^B, t_{\tau_k}] = 1$;
- 8 $Post^B[p_j^B, t_{\tau_k}] = 1$;
- 9 Let $m_0^B = \mathbf{0}^{|S| \times 1}$;
- 10 **forall** $s_i \in S_0$ **do**
- 11 $m_0^B[p_i^B] = 1$;
- 12 **forall** $s_f \in F$ **do**
- 13 $T^V = T^V \cup t_{s_f} / *$ add a new virtual transition to T^V */
- 14 Add a new column to Pre^V and to $Post^V$ corresponding to t_{s_f} ;
- 15 $Pre^V[p_f^B, t_{s_f}] = 1$;
- 16 $Post^V[p_f^B, t_{s_f}] = 1$;

y_i , one token is added to p_i^O . Therefore, if $m[p_i^O] > 0$ then observation y_i is active. Place p_i^{-O} is the complementary place of p_i^O hence is connected with the same transitions as p_i^O but with arcs oriented in the other sense. If $m[p_i^{-O}] = |R|$ then observation y_i is not active.

Finally, loop in lines 16 to 22 connect the places modeling the active and inactive observations with the transitions of the Büchi PN. Since to each transition in Büchi t_τ^B a Boolean formula (a conjunction) is assigned, each atomic proposition that appears in the proposition is connected to places in sets P^O , respectively P^{-O} , in the following way. If the atomic proposition appears not negated, then is connected with a reading arc (a bidirectional arc) to the active observation place p_i^O (line 19). On the contrary, if the atomic proposition appears negated, then is connected with a reading arc of weight $|R|$ with the inactive observation place p_i^{-O} (line 21).

Following the Alg. 3, note that transitions T^B can be fired if a set of observations are active and some are not. For example, transition t_1^B in PN of Fig. 2(b) can be executed if y_1 and y_2 are active. For this reason, transition t_1^B is connected by self-loops with places p_1^O and p_2^O . Thus, t_1^B can be fired only if the corresponding observations are active. The fired transition leads to a new marking in Q^C RMPN system.

Fig. 4 depicts a part of *Composed Petri net* with its initial marking, returned by Alg. 3. Quotient PN Q^M and Büchi PN Q^B are linked with the places representing the active and inactive observation y_3 . For the sake of clarity, Fig. 4 considers only the arcs for one region on interest (y_3). As explained in Alg. 3, when one transition in Q^M is fired and

Algorithm 3: Full PN system

Input: $Q = \langle \langle P, T, Pre, Post \rangle, m_0, \mathcal{Y}, h \rangle$,
 $B = \langle S, S_0, \Sigma_B, \rightarrow_B, F \rangle$
Output: $Q^C = \langle \langle P^C, T^C, Pre^C, Post^C \rangle, m_0^C, \mathcal{Y}, h \rangle$

- 1 Let $P^O = \{p_1^O, p_2^O, \dots, p_{|\mathcal{Y}|}^O\}$ be the set of $|\mathcal{Y}|$ places modeling the active observations;
- 2 Let $P^{-O} = \{p_1^{-O}, p_2^{-O}, \dots, p_{|\mathcal{Y}|}^{-O}\}$ be the set of $|\mathcal{Y}|$ places modeling the inactive observations;
- 3 Let $m_0^O = [0^{|P^O| \times 1}, |R| \cdot \mathbf{1}^{|P^{-O}| \times 1}]$;
- 4 Execute Alg. 1 and let $Q^M = \langle \langle P^M, T^M, Pre^M, Post^M \rangle, m_0^M, \mathcal{Y}, h \rangle$ be the returned PN;
- 5 Execute Alg. 2 and let $Q^B = \langle \langle P^B, T^B \cup T^V, [Pre^B \ Pre^V], [Post^B \ Post^V] \rangle, m_0^B, \mathcal{Y}, h \rangle$ be the returned PN;
- 6 Let $P^C = P^M \cup P^B \cup P^O \cup P^{-O}$;
- 7 Let $T^C = T^M \cup T^B \cup T^V$;
- 8 $m_0^C = [m_0^M, m_0^B, m_0^O]$;
- 9 Let $Pre^C =$

$$\begin{bmatrix} Pre^M & \mathbf{0}^{|P^M| \times |T^B|} & \mathbf{0}^{|P^M| \times |T^V|} \\ \mathbf{0}^{|P^B| \times |T^M|} & Pre^B & Pre^V \\ \mathbf{0}^{|P^O| \times |T^M|} & \mathbf{0}^{|P^O| \times |T^B|} & \mathbf{0}^{|P^O| \times |T^V|} \\ \mathbf{0}^{|P^{-O}| \times |T^M|} & \mathbf{0}^{|P^{-O}| \times |T^B|} & \mathbf{0}^{|P^{-O}| \times |T^V|} \end{bmatrix};$$
- 10 Let $Post^C =$

$$\begin{bmatrix} Post^M & \mathbf{0}^{|P^M| \times |T^B|} & \mathbf{0}^{|P^M| \times |T^V|} \\ \mathbf{0}^{|P^B| \times |T^M|} & Post^B & Post^V \\ \mathbf{0}^{|P^O| \times |T^M|} & \mathbf{0}^{|P^O| \times |T^B|} & \mathbf{0}^{|P^O| \times |T^V|} \\ \mathbf{0}^{|P^{-O}| \times |T^M|} & \mathbf{0}^{|P^{-O}| \times |T^B|} & \mathbf{0}^{|P^{-O}| \times |T^V|} \end{bmatrix};$$
- 11 **forall** $y_i \in \mathcal{Y}$ **do**
- 12 Let $P' = \{p \in P^M | y_i \in h(p)\}$;
- 13 **forall** $p_k \in P'$ **do**
- 14 $Post^C[p_i^O, \bullet p_k] = Pre^C[p_i^O, p_k \bullet] = 1$;
- 15 $Pre^C[p_i^{-O}, \bullet p_k] = Post^C[p_i^{-O}, p_k \bullet] = |R|$;
- 16 **forall** $t_\tau^B \in T^B$ **do**
- 17 Let π_i be the DNF formula assigned to t_τ^B ;
- 18 **if** $\pi_i \neq \top$ **then**
- 19 **forall atomic propositions** y_i **appearing not negated in** π_i **do**
- 20 $Pre^C[p_i^O, t_\tau^B] = Post^C[p_i^O, t_\tau^B] = 1$;
- 21 **forall atomic propositions** y_i **appearing negated in** π_i **do**
- 22 $Pre^C[p_i^{-O}, t_\tau^B] = Post^C[p_i^{-O}, t_\tau^B] = |R|$;

the observation is changed, the reduced PN of the environment deposit one token to the respective active observation, e.g., t_2^M is enabled when y_3 is not active (here the robots being in the free space initially), and if it fires a token to both p_1^M and p_3^O are produced. In Q^B , the transitions are fired based on the assigned Boolean formula. Herein, the places for active and inactive observations are required to enable these transitions, e.g., t_5^B and t_2^B depend on active observation y_3 , as it is illustrated in Fig. 4. The transitions in Büchi PN are colored

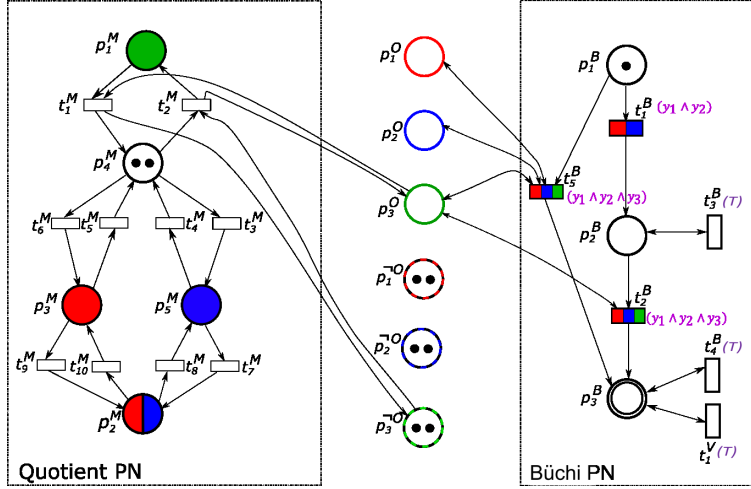


Fig. 4: Partially Composed Petri net, based on active and inactive observations of y_3

according to the required active observations, i.e., red - y_1 , blue - y_2 , green - y_3 . The rationale for the rest of connections is maintained for the active and inactive observations modeling y_1 and y_2 .

Complexity. The algorithms from the first part of the solution (designing the *Composed PN*) are tractable, being based on simple operations. Based on each algorithm's inputs, the complexity is as follows: (a) Alg. 1 is polynomial ($\mathcal{O}(n^2)$) depending on the number of places ($n = |P|$), subject to the environment decomposition technique; (b) Alg. 2 is polynomial with respect to the inputs \rightarrow_B of the Büchi automaton \mathcal{B} and the number of atomic propositions over set \mathcal{Y} . In general, the LTL formulas specified for multi-robot systems have a reduced number of atomic propositions, the exponential upper-bound of $2^{|\mathcal{Y}|}$ being seldom achieved. Lastly, (c) Alg. 3 is polynomial over cardinality of set \mathcal{Y} and of set of Büchi's transitions T^B .

VI. COMPLETE SOLUTION

This section is dedicated to return a solution in terms of robot's paths to ensure the given LTL mission. In this sense, two actions are necessary. First, a solution is obtained based on the composed PN model \mathcal{Q}^C computed previously, which captures the evolution of robots with respect to the LTL mission. Secondly, the solution is projected into the original RMPN model, outputting robots movement towards their goal positions.

Sub-Step 2.1. Solution on the reduced model. The main idea of MILP (3) is to drive the PN to a state corresponding to a final state in Büchi (marking m_{2k}^C). The solution of this MILP is divided into 2 parts, *prefix* and *suffix*, each based on the parameter k . The motivation behind the division lies in minimizing the run time for finding the full solution, since, in general, it is faster to solve two small MILP problems than a big one. The difference between these MILPs dwells in the initial marking m_0^C of *Composed Petri net* model: represented by the initial state for *prefix* and by the previously reached final state of Büchi for *suffix*.

The MILP (3) considers k steps for *prefix*, respectively *suffix*. Therefore, k is a design parameter that will correspond to the maximum number of states in *prefix* and *suffix* of accepted runs in Büchi automaton B , where $k \geq 1$. For each odd step, a transition in Quotient PN is fired, while for each even step, a transition in Büchi PN is fired. Because to create a token in a place of Büchi PN it may be necessary to move a robot through all places of the Quotient PN, an upper-bound of parameter k can be imposed, as follows: $(|P^M| - 1) \times (|P^B| - 1)$. If parameter k is chosen very small, a marking corresponding to a final state in Büchi PN cannot be reached being necessary in this case to increase k .

Explanations on MILP (3) are as follows:

- The cost function minimizes the number of fired transitions of Quotient and Büchi PNs, scaled by index i , to enforce reaching the solution during the first steps of the defined horizon of k steps, when it is possible.
- Constraints (3b) correspond to the state equation (2).
- Set of constraints (3c) allow robots to advance to only one place in Quotient PN. Note that by firing a transition in the Quotient PN, the observations are changed (or at least the regions that generate the observations) such that, in the following step (when i is even) one transition in Büchi should be fired.
- Set of constraints (3d) imposes that the first transition to fire from the Büchi PN to be different by a virtual one, thus force the Büchi to leave the initial state.
- Set of constraints (3e) allow the firing only of one transition corresponding to the Büchi PN. Notice that here, a virtual transition that has zero cost can fire also such that if the prefix or suffix is reached in a smaller steps than k , no other transitions will be executed.
- Constraints (3f) ensures the marking after k steps is the final state in Büchi, denoted as p_f^B being an input parameter.

Parameters:

- $|R|$ - number of robots
- p_f^B - place modeling a final state in Büchi
- C^C - token flow matrix of the Complete PN
- Pre^C - pre-incidence matrix of the Complete PN

Variables:

- $m_i^C = [m_i^M \ m_i^B \ m_i^O \ m_i^{-O}]$ - marking at step i of the full PN composed by the marking of Quotient PN (m_i^M), Büchi PN (m_i^B), active observation places (m_i^O) and inactive observation places (m_i^{-O});
- $\sigma_i^C = \begin{bmatrix} \sigma_i^M \\ \sigma_i^B \\ \sigma_i^V \end{bmatrix}$ - firing vector at step i of the full PN, composed by the firing vector of Quotient PN (σ_i^M), Büchi PN (σ_i^B) and of virtual transitions (σ_i^V).

Objective:

$$\min \sum_{i=1}^{2 \cdot k} i \cdot (\mathbf{1}^T \cdot \sigma_i^M + \mathbf{1}^T \cdot \sigma_i^B) \quad (3a)$$

Constraints:

$$m_i^C - m_{i-1}^C - C^C \cdot \sigma_i^C = 0, \quad i=\overline{1, 2 \cdot k} \quad (3b)$$

$$\left. \begin{array}{l} m_i^C - Pre^C \cdot \sigma_i^C \geq 0, \\ \mathbf{1}^T \cdot \sigma_i^M \leq |R|, \\ \mathbf{1}^T \cdot \sigma_i^B + \mathbf{1}^T \cdot \sigma_i^V = 0, \end{array} \right\} \quad \begin{array}{l} i=2 \cdot j+1 \\ j=\overline{0, k-1} \end{array} \quad (3c)$$

$$\left. \begin{array}{l} \mathbf{1}^T \cdot \sigma_i^M = 0, \\ \mathbf{1}^T \cdot \sigma_i^B = 1, \\ \mathbf{1}^T \cdot \sigma_i^V = 0, \end{array} \right\} \quad i=2 \quad (3d)$$

$$\left. \begin{array}{l} \mathbf{1}^T \cdot \sigma_i^M = 0, \\ \mathbf{1}^T \cdot \sigma_i^B + \mathbf{1}^T \cdot \sigma_i^V = 1, \end{array} \right\} \quad \begin{array}{l} i=2 \cdot j \\ j=\overline{2, k} \end{array} \quad (3e)$$

$$m_i^C[p_f^B] = 1, \quad i=2 \cdot k \quad (3f)$$

Sub-Step 2.2. Projecting the solution. First, from the complete solution of MILPs (3) it is extracted the sequence of markings corresponding to the robot team in the Quotient PN \mathcal{Q}^M . Let $M = \langle m_1^M, m_2^M, \dots, m_{2k}^M \rangle$ be that sequence. Before projecting the solution, the identical marking from M are removed. In particular, if $\exists m_i^M, m_{i+1}^M \in M$ such that $m_i^M = m_{i+1}^M$, then m_i^M is removed from M . The number of markings in M is, in general, reduced. Notice that only successive identical markings are removed while the marking which register the end of the *prefix* and beginning of *suffix* is stored. Additionally, let us add m_0^M as the first element in M .

Furthermore, let $G = \langle g_1, g_2, \dots, g_{2k} \rangle$ be a sequence of $2k$ vectors such that, $g_i \in \{0, 1\}^{|P^M|}$ and $g_i[j] = 1$ if $m_i^M[j] = 0$, and $g_i[j] = 0$ otherwise. This vector will be used in MILP (4) to project the solution and to not allow to activate other observation between two steps.

The following MILP extends every marking from the Quotient RMPN into a string of markings in the original RMPN. The string has the same active observations, to ensure the validity of the LTL formula when exist finite repetitions. In order to avoid collisions, a number of $|R|$ intermediate markings are additionally introduced between two successive marking, to ensure that each region of the original net is crossed by maximum one robot. Assuming that at the initial state each region contains maximum one robot, following

MILP ensures the collisions free trajectories, although the active observations are maintained.

Parameters:

- $|R|$ - number of robots
- M - sequence of markings returned by (3)
- Pr - projection matrix between Q^B and RMPN
- C - token flow matrix of the RMPN
- $Pre, Post$ - pre/post-incidence matrices of RMPN
- m_i^M - marking at step i of the Quotient PN.

Variables:

- $m_{i,j}$ - marking at step i of RMPN, considering the intermediate marking j
- $\sigma_{i,j}$ - firing vector at step i of RMPN, for the intermediate marking j with $i = \overline{0, |M|}, j = \overline{1, |R| + 1}$

Objective:

$$\min \mathbf{1}^T \cdot \sum_{i,j} \sigma_{i,j} \quad (4a)$$

Constraints:

$$m_{i,j} - m_{i,j-1} - C \cdot \sigma_i = 0, \quad i=\overline{0, |M|}, j=\overline{1, |R|+1} \quad (4b)$$

$$m_{i,0} - m_{i-1, |R|+1} = 0, \quad i=\overline{1, |M|} \quad (4c)$$

$$Pr \cdot m_{i,j} - m_i^M = 0, \quad i=\overline{0, |M|}, j=\overline{1, |R|} \quad (4d)$$

$$Post[g_i \cdot Pr, \cdot] \cdot \sigma_{i,j} = 0, \quad i=\overline{0, |M|}, j=\overline{1, |R|+1} \quad (4e)$$

$$Post \cdot \sigma_{i,j} + m_{i,j-1} \leq 1, \quad i=\overline{0, |M|}, j=\overline{1, |R|+1} \quad (4f)$$

$$m_{i, |R|+1} - Pre \cdot \sigma_{i, |R|+1} \geq 0, \quad i=\overline{0, |M|} \quad (4g)$$

The constraints in MILP (4) are the followings:

- (4b) is the state equation (2) of the RMPN model;
- (4c) ensure that the last intermediate marking is the same with the initial marking in the next step;
- (4d) keep the same observations during the $m_{i,1}$ to $m_{i, |R|}$. In fact, these $|R|$ intermediate markings are introduced in order to avoid collisions between m_i^M and m_{i+1}^M .
- Constraints (4e) ensure that the corresponding firing vectors of the intermediate markings from $m_{i,1}$ to $m_{i, |R|}$ should not activate other observations;
- (4f) ensure the collision avoidance between successive markings of the original RMPN by imposing that the number of times that each region is crossed between two intermediate markings is maximum one;
- Last constraints, (4g) impose that the movements of the robots from sub-step $m_{i, |R|}$ to sub-step $m_{i, |R|+1}$ is done synchronously by all robots (each robot fires only one transition) such that the generated observation of \mathcal{Q}^M changes according to the transitions fired in Büchi.

Global algorithm. Alg. 4 is responsible to find a complete solution for the robot trajectories, that fulfills the given mission φ . For this reason, several inputs are required as it can be seen in Alg. 4. They will be used to (i) compute a solution in the reduced model, and to (ii) project the previous solution in the original RMPN model.

The lines 3-14 search for a feasible *Run* in *Composed PN* based on MILP (3), for all places modeling the final states in Büchi (captured in set Set_f). As a first step, the *prefix* is

computed (line 5). If the *prefix* exists (line 6), then the *suffix* is computed. Let us recall that one refers to an active observation if the place p_i^O assigned to observation y_i has at least one token. Line 8 evaluates if the last active observations (denoted with P_f^O) are included in the self-loop of the final state s_f . If this condition in line 8 is respected, the *suffix* is returned by MILP (3). Otherwise, the *suffix* is represented by the final state, without being necessary to solve the MILP (3) (line 12). For both *prefix* and *suffix* not empty, the feasible *Run* is computed in line 14 which should ensure the LTL mission. Based on this *Run*, the robots trajectories are projected into the original RMPN \mathcal{Q} (line 16). If no feasible *Run* was computed for any final state in Büchi (line 19), then parameter k is increased and the procedure from lines 3-14 is performed.

In case k reaches its upper-bound and no feasible *Run* could be computed, the Alg. 4 cannot return a solution. This means that the problem does not have a solution with respect to the team of robots and the LTL mission, e.g., three disjoint regions should be visited in the same time, but the team contains two robots. This algorithm guarantees to obtain a solution if at least one exists (lines 3-14), which is correct both in terms of team capabilities and LTL satisfaction. The upper-bound of k ensure that a final state of Büchi is reached by prefix and revisited by suffix whenever possible.

Algorithm 4: Global solution for robot's trajectories

Input: RMPN \mathcal{Q} , *Composed Petri net* \mathcal{Q}^C , set \mathcal{Y} , $|R|$,
set of active observations P^O , set of final states
 $F \in B$, finite horizon k

Output: Robot movement strategies

```

1 Let  $Set_f = \{p_{f_1}^B, p_{f_2}^B, \dots, p_{f_n}^B\}$ ;
2 Let  $Run = \emptyset$ ;
3 while  $Set_f \neq \emptyset$  do
4   Select place  $p_{f_i}^B$  modeling a final state  $s_f$  in Büchi;
5   Compute prefix for  $p_{f_i}^B$  based on MILP (3);
6   if prefix  $\neq \emptyset$  then
7     Let  $P_f^O$  be the last active observations for  $p_{f_i}^B$ ;
8     if  $P_f^O \not\subseteq \pi(s_f, s_f)$  then
9       Let  $m_0^C = m_k^C$ , where  $m_k^C$  is the solution
10      of MILP (3);
11      Compute suffix based on MILP (3);
12    else
13       $suffix = s_f$ ;
14  if (prefix  $\neq \emptyset$  AND suffix  $\neq \emptyset$ ) then
15     $Run = prefix \ suffix \ suffix \dots$ ;
16 if  $Run \neq \emptyset$  then
17   Compute Robot movement strategies based on
18   MILP (4) for the returned Run;
19 else if  $k < ((|P^M| - 1) \times (|P^B| - 1))$  then
20   Increase parameter  $k$ ;
21   Compute Run for new  $k$  /* lines 3-14 */
22 else
23   Return false. The formula cannot be achieved by
24   the robots in the actual environment.
```

It is worth mentioning that our approach has a slower increase of complexity than other methods which are based on a product of automata. Herein, the maximum number of places in the *Composed Petri net* \mathcal{Q}^C is given by the sum of places for \mathcal{Q}^M , the number of places for \mathcal{Q}^B and twice the number of ROIs, $2 \cdot |\mathcal{Y}|$. Thus, the state explosion problem is avoided. Although optimality is not achieved in terms of trajectories length or number of firings in the original RMPN for a single repetition of suffix, the solution obtained in the reduced model can be improved by considering all the final states s_f in Alg. 4 while choosing a desired run rather than stopping at the first obtained one.

Complexity. The complexity of this algorithm is NP-hard, justified by the use of MILP problems. The total number of unknown variables in both MILPs is given by the number of markings and transitions in \mathcal{Q}^C , respectively the number of markings and transitions in \mathcal{Q} . On the other hand, the total number of constraints is related to the number of intermediate markings for MILP (3), while MILP (4) depends on the solution of the previous MILP.

VII. SIMULATION RESULTS AND COMPARISON TO [1]

The solution proposed in this paper was implemented and integrated in RMTTool - MATLAB [35], using the CPLEX Optimizer [36] solver for the mentioned MILPs from the previous section. The results captured in this section were obtained using a laptop with i7 - 8th gen. CPU @ 2.20GHz and 8GB RAM.

Example 7.1: Let us recall the environment from Fig. 1 (a) and the LTL mission that needs to be fulfilled, as in equation (1):

$$\varphi = \diamond (y_1 \wedge y_2 \wedge y_3) \wedge \neg (y_1 \vee y_2) \mathcal{U} (y_1 \wedge y_2).$$

The robots need to reach all three regions of interest at the same time, ensuring y_1 and y_2 are reached simultaneously. Figure 1(a) illustrates the robot trajectories returned by Alg. 4. It can be observed that both robots moves towards the regions y_1 and y_2 to complete the concurrently requirement. Afterwards, one of the robots (r_1) advances and enters the last region of interest y_3 , while the second robot enters $p_{13} = \{y_1, y_2\}$ in the same time. Several numerical results can be specified, based on the described steps in Section V, such as: the resulting *Quotient PN model* with 5 places and 10 transitions computed in 0.02 seconds, the *Büchi automaton* with 3 states returned in 0.16 seconds and the *Composed PN model* with 14 places and 16 transitions (in account of the added virtual transition) computed in 0.02 seconds. MILP (3) reaches the final state in Büchi in 0.05 seconds, using 180 unknown variables (for $k = 6$). The MILP (3) returns the *prefix* $s_1 s_2$, without the necessity of solving MILP (3) to compute the *suffix*, because the final state s_3 is True \top for its self-loop. The last phase of the complete algorithm lies in projecting the solution returned so far in the original RMPN, based on MILP (4). The run time is 0.05 seconds for 900 unknown variables, with the cost function equal with 11 (minimum number of cells crossed by the robots).

Notice that with the inclusion of virtual transitions connected with the final states, the minimum value of MILP (3) is independent of the value of k parameter. ■

The result analysis is based on a comparison of the current approach from Alg. 4 - joined model of *Composed Petri net* model, in contrast with the sequential procedure of the two models PN and Büchi automaton, captured in [1]. We will refer to the first approach as *with Büchi*, while the second approach will be denoted as *following Büchi*. The comparison does not include methods based on discrete transition systems by cause of the state explosion problem. As a reminder, the method from [1] consist in a iteration of a finite number of acceptable runs in Büchi automaton which satisfy the LTL formula. Then it examines the sequence of reachable markings for which the desired observations can be activated, while respecting the desired run. Both works acknowledge the benefits of Büchi automaton model and Petri net models, while maintaining the collision avoidance between the robots. Nevertheless, the contribution of the current method prevail a complete algorithm, based on the joined model \mathcal{Q}^C . It should be noted that the collision avoidance problem is solved in [1] only when several restrictions make good use of a parameter with a suitable chosen value. Otherwise, the collision free trajectories cannot be guaranteed. On the other hand, the current approach solves this problem based only on the set of restrictions (4f) of MILP (4).

Example 7.2: We consider the next LTL formula, by maintaining the synchronization operation illustrated previously: $\varphi = \square(\diamond y_1 \wedge \diamond y_3 \wedge \diamond y_5 \wedge \diamond y_6 \wedge \diamond y_7 \wedge \diamond y_8) \wedge \neg(y_5 \vee y_6) \mathcal{U}(y_5 \wedge y_6) \wedge \neg(y_4 \vee y_7) \mathcal{U}(y_4 \wedge y_7)$. This specification imposes the visit of several ROIs in an environment with 8 regions of interest, while the regions y_5 and y_6 are simultaneously reached, respectively y_4 and y_7 . Table II captures the comparison between the mentioned methods in terms of running time and value of the cost function (number of crossed cells following the robot trajectories). The table accounts scenarios with 4, 5, 6 and 10 robots, and Fig. 5 exemplifies robots trajectories for 6 robots. The synchronization points for the entire team (black stars) are depicted along the trajectories right before entering a regions of interest. Both approaches consider an equal the number of intermediate markings ($k = 10$).

TABLE II: Comparison between current approach *with Büchi* and *following Büchi* captured in [1].

Number of robots	Run time to return a solution [sec]		Cost function value	
	<i>following Büchi</i>	<i>with Büchi</i>	<i>following Büchi</i>	<i>with Büchi</i>
4	9.56	0.75	37	39
5	2.22	0.26	23	28
6	0.77	0.11	20	21
10	1.2	0.78	13	13

The procedure *with Büchi* returns the solution for a RMPN model with 37 places and 67 transitions, and the procedure *following Büchi* computes the solution for RMPN model with 62 places and 182 transitions. The running time for the current

method is smaller than the previous approach, as a result of solution division in *prefix* and *suffix*. For the example illustrated in Fig. 5, the MILP (3) assigned to *suffix* is not computed, by cause of last active observations being included in the self-loop of the final state in Büchi. ■

Let us recall the meaning of the cost function for MILP (4) as being the total number of fired transitions in the original RMPN model. Although in the table it can be seen that the current approach returns a cost function value bigger or equal compared with the method from [1], this fact is not always true. Let us consider the counterexample with the LTL formula: $\varphi = \diamond y_2 \wedge \square \diamond (y_1 \wedge \diamond y_3) \wedge \neg y_3 \mathcal{U} y_2$ applied for the same environment from Fig. 1. Informally, this requirement specifies the visit of region y_2 before y_3 sometime along the trajectory and the visit of y_1 and y_3 infinitely often. In this sense, a certain order for visiting the ROIs is imposed. After running the Alg. 4, the complete solution is obtained 0.05 seconds by solving both MILPs (3 and 4) for the joined model \mathcal{Q}^C with 19 places and 36 transitions. The Büchi automaton of the LTL specification contains two final states, for each of those returning the cost function 6, respectively 10. The current method projects the solution for the final state with the smaller cost function (6), while the method *following Büchi* returns the cost function equal with 10.

VIII. CONCLUSION

This paper proposes a complete algorithm in terms of motion planning for dynamic multi-robot systems. A global LTL specification is given for a team of identical robots, which should reach and/or avoid several regions of interest in the environment. Two formalisms are used for the collision free trajectories: (1) Robot Motion Petri net (RMPN) model for to the environment, and (2) Büchi automaton for the LTL formula. The proposed algorithm values the advantages of both models by a joint new representation denoted *Composed Petri net* system.

The efficiency of both the proposed *Composed Petri net* model and the complete algorithm were illustrated in the numerical evaluation, considering a comparison with a previous work [1]. The current method offers a complete solution based on the union of both models (environment and mission), in contrast with the previous work based on iterative and sequential approach of the models which cannot assure the completeness in terms of robot trajectories. In addition, the method proves to increase slower in terms of complexity (run time) compared with techniques based on automaton products, in account of a smaller number of places in the *Composed PN*.

The future work envisions to further reduce the complexity, while considering partial unknown environment. One approach in this sense is based on distributive algorithms in comparison with the centralized current method, e.g., each robot computes its own trajectory.

REFERENCES

- [1] M. Kloetzer and C. Mahulea, "Path planning for robotic teams based on LTL specifications and Petri net models," *Discrete Event Dynamic Systems*, vol. 30, no. 1, pp. 55–79, 2020.

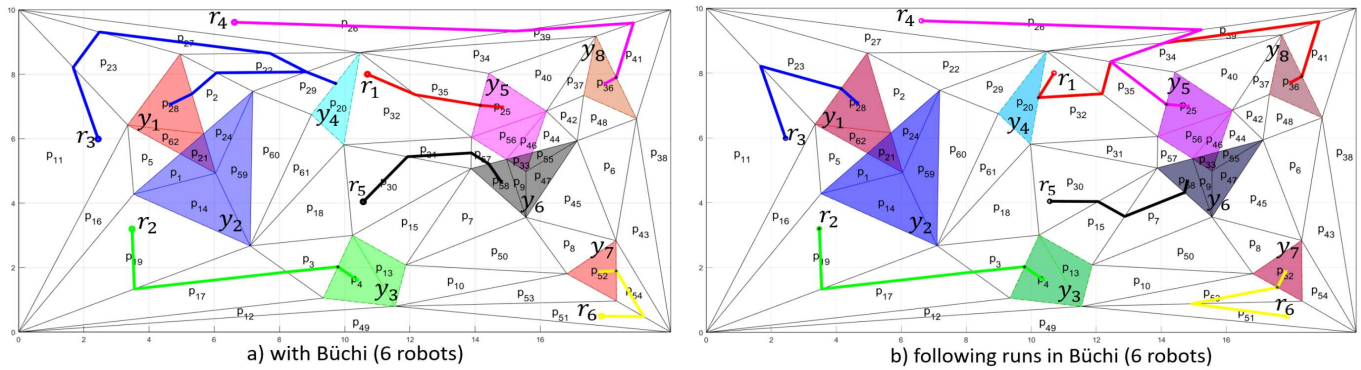


Fig. 5: Trajectories satisfying the LTL formula from Example 7.2 (red - r_1 ; green - r_2 , blue - r_3 , magenta - r_4 , black - r_5 , yellow - r_6)

- [2] J. Tumova and D. V. Dimarogonas, "Multi-agent planning under local LTL specifications and event-based synchronization," *Automatica*, vol. 70, pp. 239–248, 2016.
- [3] P. Yu and D. V. Dimarogonas, "Distributed motion coordination for multi-robot systems under LTL specifications," *arXiv preprint arXiv:2103.09111*, 2021.
- [4] E. Montijano and C. Mahulea, "Probabilistic Multi-Robot Path Planning with High-Level Specifications using Petri Net Models," in *2021 IEEE 17th International Conference on Automation Science and Engineering (CASE)*. IEEE, 2021, pp. 2188–2193.
- [5] B. Lacerda and P. U. Lima, "Petri net based multi-robot task coordination from temporal logic specifications," *Robotics and Autonomous Systems*, vol. 122, pp. 343–352, 2019.
- [6] C. Mahulea, M. Kloetzer, and J.-J. Lesage, "Multi-robot path planning with boolean specifications and collision avoidance," *IFAC-PapersOnLine*, vol. 53, no. 4, pp. 101–108, 2020.
- [7] M. H. Cohen and C. Belta, "Model-based reinforcement learning for approximate optimal control with temporal logic specifications," in *Proceedings of the 24th International Conference on Hybrid Systems: Computation and Control*, 2021, pp. 1–11.
- [8] X. C. Ding, M. Kloetzer, Y. Chen, and C. Belta, "Automatic deployment of robotic teams," *IEEE Robotics & Automation Magazine*, vol. 18, no. 3, pp. 75–86, 2011.
- [9] S. M. LaValle, *Planning algorithms*. Cambridge university press, 2006.
- [10] J. Esparza, J. Křetínský, and S. Sickert, "One theorem to rule them all: A unified translation of LTL into ω -automata," in *33rd Annual ACM/IEEE Symposium on Logic in Computer Science*, 2018, pp. 384–393.
- [11] I. Hustiu, M. Kloetzer, and C. Mahulea, "Distributed path planning of mobile robots with LTL specifications," in *2020 24th International Conference on System Theory, Control and Computing (ICSTCC)*. IEEE, 2020, pp. 60–65.
- [12] S. Hustiu, I. Hustiu, M. Kloetzer, and C. Mahulea, "LTL Task Decomposition for 3D High-Level Path Planning," *Journal of Control Engineering and Applied Informatics*, vol. 23, no. 3, pp. 76–87, 2021.
- [13] M. Guo and D. V. Dimarogonas, "Multi-agent plan reconfiguration under local LTL specifications," *The International Journal of Robotics Research*, vol. 34, no. 2, pp. 218–235, 2015.
- [14] E. M. Wolff, U. Topcu, and R. M. Murray, "Optimization-based trajectory generation with linear temporal logic specifications," in *2014 IEEE International Conference on Robotics and Automation (ICRA)*. IEEE, 2014, pp. 5319–5325.
- [15] R. Dimitrova, M. Ghasemi, and U. Topcu, "Maximum realizability for linear temporal logic specifications," in *International Symposium on Automated Technology for Verification and Analysis*. Springer, 2018, pp. 458–475.
- [16] C. Mahulea, M. Kloetzer, and R. González, *Path Planning of Cooperative Mobile Robots Using Discrete Event Models*. Wiley-IEEE Press, 2020.
- [17] P. Tabuada, G. J. Pappas, and P. Lima, "Motion feasibility of multi-agent formations," *IEEE Transactions on robotics*, vol. 21, no. 3, pp. 387–392, 2005.
- [18] H. Costelha and P. Lima, "Robot task plan representation by Petri nets: modelling, identification, analysis and execution," *Autonomous Robots*, vol. 33, no. 4, pp. 337–360, 2012.
- [19] B. Lacerda and P. U. Lima, "LTL-based decentralized supervisory control of multi-robot tasks modelled as Petri nets," in *2011 IEEE/RSJ International Conference on Intelligent Robots and Systems*. IEEE, 2011, pp. 3081–3086.
- [20] X. Dai, L. Jiang, and Y. Zhao, "Cooperative exploration based on supervisory control of multi-robot systems," *Applied Intelligence*, vol. 45, no. 1, pp. 18–29, 2016.
- [21] B. Lacerda and P. U. Lima, "Petri net based multi-robot task coordination from temporal logic specifications," *Robotics and Autonomous Systems*, vol. 122, p. 103289, 2019.
- [22] H. Choset, K. M. Lynch, S. Hutchinson, G. Kantor, W. Burgard, L. E. Kavraki, and S. Thrun, *Principles of Robot Motion: Theory, Algorithms, and Implementations*. Boston: MIT Press, 2005.
- [23] L. C. G. J. M. Habets, P. J. Collins, and J. H. van Schuppen, "Reachability and control synthesis for piecewise-affine hybrid systems on simplices," *IEEE Transactions on Automatic Control*, vol. 51, pp. 938–948, 2006.
- [24] C. Belta and L. Habets, "Controlling a class of nonlinear systems on rectangles," *IEEE Transactions on Automatic Control*, vol. 51, no. 11, pp. 1749–1759, 2006.
- [25] E. M. M. Clarke, D. Peled, and O. Grumberg, *Model checking*. MIT Press, 1999.
- [26] C. Baier and J.-P. Katoen, *Principles of model checking*. MIT Press, 2008.
- [27] C. Belta, A. Bicchi, M. Egerstedt, E. Frazzoli, E. Klavins, and G. Pappas, "Symbolic planning and control of robot motion," *IEEE Robotics and Automation Magazine*, vol. 14, no. 1, pp. 61–71, 2007.
- [28] G. E. Fainekos, A. Girard, H. Kress-Gazit, and G. J. Pappas, "Temporal logic motion planning for dynamic robots," *Automatica*, vol. 45, no. 2, pp. 343–352, 2009.
- [29] P. Wolper, M. Vardi, and A. Sistla, "Reasoning about infinite computation paths," in *Proceedings of the 24th IEEE Symposium on Foundations of Computer Science*, E. N. et al., Ed., Tucson, AZ, 1983, pp. 185–194.
- [30] G. Holzmann, *The Spin Model Checker, Primer and Reference Manual*. Reading, Massachusetts: Addison-Wesley, 2004.
- [31] P. Gastin and D. Oddoux, "Fast LTL to Büchi automata translation," in *Proceedings of the 13th Conference on Computer Aided Verification (CAV'01)*, ser. LNCS, H. C. G. Berry and A. Finkel, Eds., no. 2102. SPRINGER, 2001, pp. 53–65.
- [32] A. Duret-Lutz, A. Lewkowicz, A. Fauchille, T. Michaud, E. Renault, and L. Xu, "Spot 2.0 - a framework for LTL and ω -automata manipulation," in *In: Proc. of ATVA'16*, ser. LNCS, no. 9938, 2016, pp. 122–129.
- [33] K. Etessami, "Stutter-invariant languages, ω -automata, and temporal logic," in *International Conference on Computer Aided Verification*. Springer, 1999, pp. 236–248.
- [34] E. Vitolo, C. Mahulea, and M. Kloetzer, "A computationally efficient solution for path planning of mobile robots with boolean specifications," in *ICSTCC'2017: 21st International Conference on System Theory, Control and Computing*, Sinaia, Romania, 2017, pp. 63–69.
- [35] R. González, C. Mahulea, and M. Kloetzer, "A matlab-based interactive simulator for mobile robotics," in *IEEE CASE'2015: Int. Conf. on Autom. Science and Engineering*, 2015.
- [36] IBM, "IBM ILOG CPLEX Optimization Studio. Software," <https://www.ibm.com/es-es/products/ilog-cplex-optimization-studio>, 2016.



Sofia Hustiu received the B.S. and M.Sc. degrees in automatic control and applied informatics from the Technical University of Iasi, Romania, in 2018, respectively 2020. She is currently a Ph.D. student in a joint program between University of Zaragoza, Spain and Technical University of Iasi, Romania. In the academic year 2021-2022 she benefits from an ERASMUS+ program, as well as a 3-month research stay at KTH Royal Institute of Technology in Stockholm, Sweden. Her research interests include path planning and task assignment for multi-agent

systems based on discrete event systems and high-level specifications.

Sofia Hustiu is a teaching assistant at Technical University of Iasi, Romania, for the following fields: introduction in control system theory, statistics and path planning strategies for multi-agent systems.



Cristian Mahulea received the B.S. and M.Sc. degrees in control engineering from the "Gheorghe Asachi" Technical University of Iasi (Romania), in 2001 and 2002, respectively, and Ph.D. degree in systems engineering from the University of Zaragoza (Spain) in 2007. He is an Associate Professor and head of the Department of Computer Science and Systems Engineering at the University of Zaragoza, Spain. His research interests include discrete event systems, hybrid systems, automated manufacturing, Petri nets, mobile robotics and healthcare systems.

He participated in the development of **Petri Net Toolbox** for the simulation, analysis and synthesis of discrete-event systems modeled with discrete Petri nets and **RMTool** for path planning and motion control of mobile robots.

He was visiting professor at the University of Cagliari (Italy) with the Department of Electrical and Electronic Engineering during five months in 2008 and 2010 and a Visiting Researcher at the University of Sheffield (U.K.), University of Cagliari (Italy), Boston University (USA) and ENS Paris-Saclay (France). He has been General Chair of ETFA'2019 being Program Committee chair of ETFA'2017 and ETFA'2018. As editorial activities, Cristian was Associate Editor of IEEE Transactions on Automation Science and Engineering (TASE), and currently he is an Associate Editor of IEEE Control Systems Letters (L-CSS) and of IEEE Transactions on Automatic Control (TAC).



Marius Kloetzer received the B.S. and M.Sc. degrees in computer science from the Technical University of Iasi, Romania, in 2002 and 2003, respectively, and the Ph.D. degree in systems engineering from Boston University, MA, USA, in 2008. He is currently a Full Professor with the Technical University of Iasi, Romania. His research interests include formal tools for discrete event systems with applications in motion planning for mobile robots.

Marius Kloetzer was a visiting researcher at Ghent University, Belgium, and at University of Zaragoza,

Spain. He has been Organizing Committee chair at ICSTCC'2017 and Work-in-Progress co-chair at ETFA'2019.



Jean-Jacques Lesage received the Ph.D. degree from the Ecole Centrale de Paris, France, and the Habilitation à Diriger des Recherches from the University of Nancy, France, in 1989 and 1994 respectively. Currently, he is Professor of Automatic Control with the Ecole Normale Supérieure Paris-Saclay, France. His research interests include formal methods and models for identification, analysis and diagnosis of Discrete Event Systems, as well as applications to manufacturing systems, network automated systems, energy production, and more

recently ambient assisted living.